Noise Removal and Contrast Enhancement for X-Ray Images

[1]Ren-You Huang, [2]Lan-Rong Dung, [3]Cheng-Fa Chu and [4]Yin-Yi Wu
[1]Institute of Electrical Control Engineering, National Chiao Tung University, Taiwan;
[2,3]Department of Electrical and Computer Engineering, National Chiao Tung University, Taiwan;
[4]National Chung-Shan Institute of Science and Technology, Taiwan;
hry76519@gmail.com; lennon@faculty.nctu.edu.tw; cfc310186.eed00g@nctu.edu.tw;
davidwu0801@gmail.com

ABSTRACT

X-ray image plays a very important role in the medical diagnosis. To help the doctors for diagnosis of the disease, some algorithms for enhancing X-ray images were proposed in the past decades. However, the enhancement of images will also amplify the noise or produce distortion of image, which are unfavorable to the diagnosis. Therefore, appropriate techniques for noise suppression and contrast enhancement are necessary. This paper proposed an algorithm including two-stage filtering and contrast enhancement for X-ray images. By using adaptive median filter and bilateral filter, our method is able to suppress the mixed noise which contains Gaussian noise and impulsive noise, while preserving the important structures (e.g., edges) in the images. Afterwards, the contrast of image is enhanced by using gray-level morphology and contrast limited histogram equalization (CLAHE). In the experiments, we evaluate the performance of noise removal and contrast enhancement separately with quantitative indexes and visual results. For the mixed noise case, our method is able to achieve averaged PSNR 39.89 dB and averaged SSIM 0.9449; for the contrast enhancement, our method is able to enhance more detail structures (e.g., edges, textures) than CLAHE.

Keywords: Medical Image Processing; Noise Reduction; Contrast Enhancement; X-ray images.

1   Introduction

X-ray imaging has been widely used in the real-world applications, for instance, medical diagnosis, customs inspection. The X-ray images are especially common way to aid the doctors in diagnosing the diseases of patients. The proper visual characteristics which determine the quality of X-ray images are density and contrast [1]. However, the contrast of X-ray images is usually low, which may influence the doctors' diagnosis. Besides, the noises that accompany the low contrast X-ray images will also degrade the image quality. In the following, we will briefly review the classical methods of noise removal and contrast enhancement.

The previous works applied different denoising methods for different noise types. For example, using Gaussian filter [2], anisotropic diffusion [3-5], or bilateral filters [6, 7], to deal with the Gaussian noise; or using median filters [8-11] to deal with the impulsive noises (like salt and pepper), which are produced by corrupted pixels. The Gaussian filter is a kind of mean filter with the Gaussian distributed weightings instead of equal ones. The anisotropic diffusion solves the partial differential equation iteratively. The

bilateral filter computes the distance weight and similarity weight of the pixels in the filter window. Both the anisotropic diffusion and bilateral filter can preserve the edges while reducing the noise. The median filter is a non-linear filter which replaces the center pixel with the median value within the filter window.

To enhance the contrast of images, typical methods are based on the histogram equalization [12-22]. The histogram equalization enhances the contrast by remapping the intensity of the images from original distributions to the more uniform ones [12-14, 17, 18]. However, using histogram equalization may amplify the noise at the same time. Moreover, for some images with uniformly distributed histogram, the histogram equalization will show limited enhancement of the contrast. The adaptive histogram equalization can enhance the local contrast, which is more robust to the noise than the histogram equalization, and is able to obtain more visually satisfactory results [15, 19-22].

Recent works show impressive results of medical image enhancement [3, 23, 24]. Yang et al. [23] proposed an approach based on wavelet transform for medical image enhancement. Vibhakar et al. [24] applied five widely used techniques to enhance the medical images, including spatial domain filtering, frequency domain filtering, histogram processing, morphological filtering and wavelet-based filtering. Kurt et al. [3] proposed a hybrid algorithm which includes mathematical morphology, anisotropic diffusion filter and contrast limited adaptive histogram equalization (CLAHE).

This paper proposed an algorithm for X-ray image enhancement which can reduce the mixed noises and enhance the contrast. We first remove the impulsive noise by adaptive median filter, which are only applied to the pixels detected as impulsive noises. The bilateral filter is applied to the image to reduce the Gaussian noises. Then, we perform two gray-level morphology techniques (top-hat and bottom-hat transform) to the image, followed by the CLAHE algorithm, to enhance the contrast of the image.

2   The Proposed Method

Figure 1 shows the flow chart of the proposed algorithm, which includes: adaptive median filter, bilateral filter, mathematical morphology, and contrast limited histogram equalization. The details of each part are described in the following subsections.
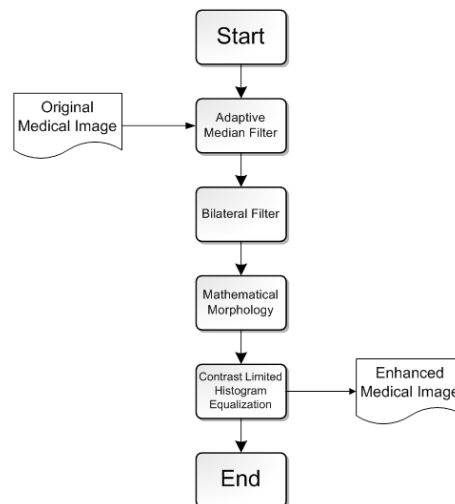

Figure 1. The processing flow of the proposed algorithm.

2.1 Adaptive median filter

The adaptive median filter [11] had been proposed as an improved version of traditional median filtering, which mainly contains two parts: noise detection and median filtering with adjustable window size. The noise detection determines whether a pixel is corrupted by impulsive noise or not. The median filter is then only applied to the noise pixel, which can reduce the computational cost. To determine the noise pixels, we defined a simple criterion as follows:

$$\left| I(x,y) - \overline{I}_{x,y} \right| > T_1 \tag{1}$$

where I(x,y) is an image pixel at (x, y), $\overline{I}_{x,y}$ is the mean value of the pixels within a n × n window centered at (x, y), and T_1 is the predefined threshold. With this simple noise detection, the further processing is only applied to the detected noise pixels, thus the computational cost can be reduced.

The traditional median filter is suitable for the impulsive noise (e.g., salt-and-pepper noise). However, it is possible that the median value of the pixels within a fixed window is still one of the noise pixels if the window size is small. On the other hand, one may lose the detail information or structure of an image if the window size is large. To avoid these problems, the window size should be adjustable according to the noise level and content of image. Figure 2 shows the flow chart of the adaptive median filter, where W_{xy} is the window centered at (x, y), T_2 is the predefined threshold, and I_{min}, I_{med}, I_{max} are minimum, median, maximum values within the window W_{xy}.
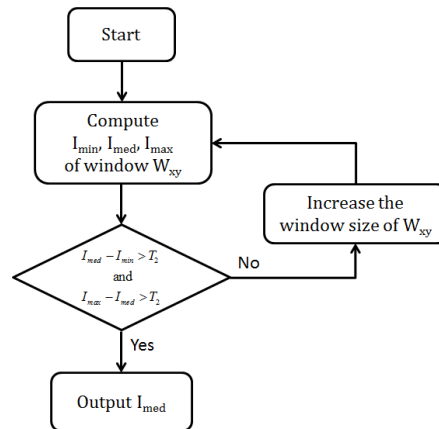

Figure2. The flow chart of the median filter with adjustable window size.

2.2 Bilateral filter

The adaptive median filter is able to handle the dense impulsive noise, however, it still shows limited success to handle the Gaussian noise. To reduce the Gaussian noise effectively, we applied the bilateral filter [7] as the complement part of adaptive median filter.

Bilateral filter is a non-linear filter which takes both the spatial distance and pixel similarity into considerations. The bilateral filtered result of a pixel I_c is computed as follows:

$$I_c' = \frac{\sum_{q \in W} f\left(\left|c - q\right|\right) g\left(\left|I_c - I_q\right|\right) I_q}{\sum_{q \in W} f\left(\left|c - q\right|\right) g\left(\left|I_c - I_q\right|\right)} \tag{2}$$

where W is the window centered at position c, f (.) is the spatial weighting function, and g(.) is the similarity weighting function. Typically, both the spatial and similarity weighting functions are Gaussian kernels, which are defined as follows:

$$f\left(\left|c-q\right|\right) = Ae^{-\frac{\left|c-q\right|^2}{2\sigma_f^2}} \tag{3}$$

$$g\left(\left|I_c-I_q\right|\right) = Be^{-\frac{\left|I_c-I_q\right|^2}{2\sigma_g^2}} \tag{4}$$

Where A and B are normalization constants, σ_f^2 and σ_g^2 are the variances of the Gaussian kernels.

Unlike the traditional spatial filter (e.g., Gaussian filter, mean filter) which may blur the edges of image, bilateral filter is able to effectively reduce the Gaussian noise while preserving the edges of image since it takes pixel similarity into consideration. The pixels which are dissimilar to the center pixel will have small weightings in Eq. (2), thus the edges will not be blurred.

2.3 Mathematical morphology

Mathematical morphology [25] is a branch of nonlinear filters, which is usually used to address the image sharpening problem [26]. We applied top-hat and bottom-hat transform in our morphological processing, which can extract the features of a gray scale image. The top-hat transform and the bottom-hat transform of an image can be defined as follows:

$$I_{top} = I - \left(I \circ b\right) \tag{5}$$

$$I_{bottom} = \left(I \bullet b\right) - I \tag{6}$$

where ∘ is the gray scale "opening" operator, • is the gray scale "closing" operator, and b is the structure element. The opening operation is used to emphasize the features with darker gray scales, while the closing operation is used to emphasize the features with brighter gray scales. Therefore, by taking the difference between the original image and its opening and closing versions in Eq. (5) and Eq. (6), it is clear that the top-hat transform can extract the brighter features and the bottom-hat transform can extract the brighter features.

After we obtained the top-hat and bottom-hat of the image, we combined the image and its top-hat and bottom-hat transformed versions to create an enhanced image:

$$I_{new} = I + I_{top} - I_{bottom} \tag{7}$$

The top-hat transform extracts the peaks and ridges which were removed by the opening operation, thus adding these features to the original image is able to enhance brighter structures; on the other hand, the bottom-hat transform extracts the valleys and troughs which were removed by closing operation, thus subtracting these features is able to enhance the darker structures (i.e., made the darker features even darker).

2.4 Contrast limited adaptive histogram equalization

Pizar et al. [15] proposed the "Contrast limited adaptive histogram equalization" (CLAHE) as the improved version of adaptive histogram equalization (AHE). The AHE computes the histogram of a local window centered to determine the mapping function for the local region, which results in local contrast enhancement. However, AHE may amplify the noise in homogeneous region due to the large slope of mapping function. On the contrary, the CLAHE restricts the slope of mapping function which is able to reduce the undesired amplification of noise in homogeneous region. Since there are many homogeneous regions in medical images, thus the CLAHE is suitable for enhancing medical images.

First, the image is divided into several non-overlapping regions with equal size, and the histograms of each region are then calculated. To restrict the slope of mapping function, the clip-limit β is defined as follows:

$$\beta = \frac{M}{256}\left(1 + \frac{\alpha}{100}\left(s_{max} - 1\right)\right) \tag{8}$$

where M is the number of pixels in a region, α is the clip factor within the range of [0, 100], and s_{max} is the maximum slope which is typically in the range of [1, 4]. The histogram bins with the pixel counts exceeding the clip-limit are redistributed to all bins equally, as shown in Figure 3. This process will repeat until there is no histogram bin with pixel count exceeding the clip-limit. Next, the redistributed histograms of each region are used to compute their own mapping functions for the traditional histogram equalization. Finally, each pixel of image is obtained by using bilinear interpolation based on its remapped values from mapping functions of neighbor regions. For more details of CLAHE, please refer to [15].
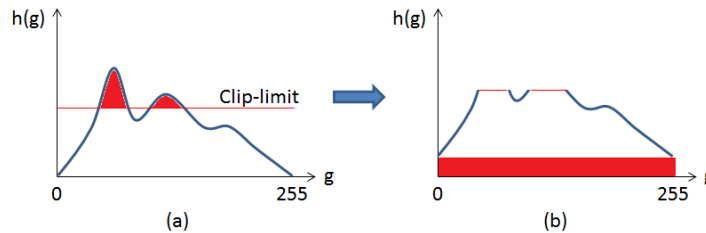

Figure 3. The illustration of histogram redistribution in CLAHE. (a) The original histogram. (b) The redistributed histogram.

3   Results and Discussions

3.1 Experimental setup

In the experiments, we test five X-ray images with low contrast, as shown in Figure 4, to evaluate the performance of different methods. We evaluated the performance of noise removal and contrast enhancement independently since the noise removal and contrast enhancement are two separate issues. To evaluate the performance of noise removal, we tested three cases: (1) adding the Gaussian noise with standard deviation 10 to the images; (2) adding the salt-and-pepper noise with probability 10% to the images; (3) adding both the noises to the images. We compared our method with adaptive median filter, bilateral filter, and the method proposed by Kurt et al. [3], in the experiments of noise

removal. Then we compared our method with AHE and CLAHE in the experiments of contrast enhancement. The parameters in our method are: T_1 = 8, T_2 = 3, σ_f = 2, σ_g = 12, s_{max} = 4, and α = 1, respectively. We fixed all the parameters for all the images in the experiments.
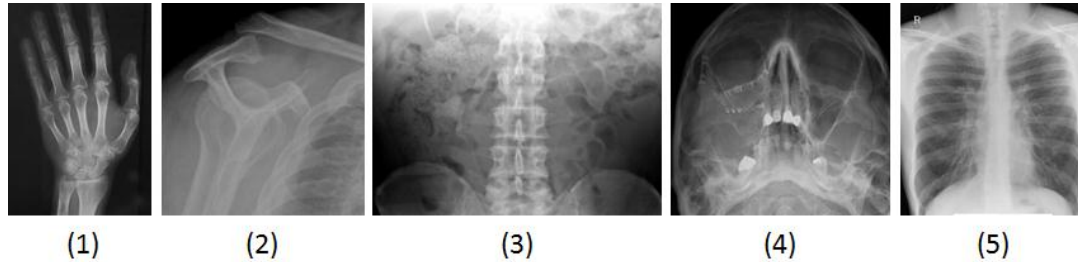

Figure 4. The test images used in the experiments.

3.2 Evaluation of noise removal

To evaluate the results objectively, we use two quantitative indexes, which are peak signal-to-noise ratio (PSNR) and structural similarity (SSIM), in the noise removal experiments. These two indexes are computed as follows:

$$PSNR(X,Y) = 10 \cdot \log_{10}\left(\frac{255^2}{MSE(X,Y)}\right) \tag{9}$$

$$SSIM(X,Y) = \frac{1}{N}\sum_{i=1}^{N}\frac{\left(2\mu_{x,i}\mu_{y,i}+c_1\right)\left(2\sigma_{xy,i}^2+c_2\right)}{\left(\mu_{x,i}^2+\mu_{y,i}^2+c_1\right)\left(\sigma_{x,i}^2+\sigma_{y,i}^2+c_2\right)} \tag{10}$$

where X is the denoised image and Y is the original image; MSE(·) is the mean square difference between two images; N is the number of pixels; i is the pixel index; $\mu_{x,i}$ and $\mu_{y,i}$ are the mean values of a local window centered at pixel i; $\sigma_{x,i}$ and $\sigma_{y,i}$ are standard deviations, and $\sigma_{xy,i}^2$ is the covariance; c_1 and c_2 are constants.

We first tested the images with Gaussian noise. Table 1 and Table 2 show the PSNR and SSIM of the images denoised by different methods. Bilateral filter is able to deal with the Gaussian noise, therefore, the PSNR and SSIM is higher than the other two. Our method combines the adaptive median filter and bilateral filter such that the results of our method are close to the results of bilateral filter.

Table 1. PSNR (dB) of the denoised images with Gaussian noise

Images	Adaptive median filter	Bilateral filter	[3]	Our method
1	35.04	41.72	36.81	41.40
2	35.22	42.10	40.16	42.11
3	35.10	41.95	40.36	41.96
4	35.70	38.87	36.19	38.66
5	35.29	39.61	35.63	41.73
Average	35.27	40.85	37.83	41.17

We then tested the images with impulsive noise, i.e., salt-and-pepper noise. Table 3 and Table 4 show the PSNR and SSIM of the images denoised by different methods. In this case, the adaptive median filter outperforms the other two. Since our method contains the adaptive median filter, therefore, in this case, the performance of our method is very close to the adaptive median filter.

Table 2. SSIM of the denoised images with Gaussian noise

Images	Adaptive median filter	Bilateral filter	[3]	Our method
1	0.8017	0.9683	0.9341	0.9686
2	0.7754	0.9315	0.9026	0.9339
3	0.8028	0.9602	0.9469	0.9617
4	0.8410	0.9165	0.8779	0.9145
5	0.8437	0.9661	0.9492	0.9662
Average	0.8129	0.9485	0.9221	0.9490

Table 3. PSNR (dB) of the denoised images with salt-and-pepper noise

Images	Adaptive median filter	Bilateral filter	[3]	Our method
1	52.32	24.57	26.44	51.42
2	55.36	25.40	31.96	52.80
3	55.70	25.12	29.43	53.40
4	46.11	24.77	29.15	45.71
5	43.15	25.34	31.21	43.01
Average	50.53	25.04	29.64	49.27

Table 4. SSIM of the denoised images with salt-and-pepper noise

Images	Adaptive median filter	Bilateral filter	[3]	Our method
1	0.9982	0.7240	0.8336	0.9973
2	0.9975	0.6881	0.9377	0.9955
3	0.9981	0.7129	0.9074	0.9966
4	0.9889	0.9165	0.8697	0.9870
5	0.9973	0.6959	0.9346	0.9961
Average	0.9960	0.7475	0.8966	0.9945

Finally, we tested the images with mixed noises. Table 5 and Table 6 show the PSNR and SSIM of the results of different methods. In this case, our method significantly outperforms the other three methods since we combine the adaptive median filters and bilateral filter such that even the mixed noise can be removed effectively without distorting the image structure. Our method obtained averaged PSNR 40.49 dB and averaged SSIM 0.9469, which outperforms the PSNR of adaptive median filter (35.92 dB) and the SSIM of [3] (0.8655). For visual evaluation, Figure 5 shows an example of the denoised results in the mixed-noise case. We can observe that our method obtain the result with least noise which is most similar to the original image.

Table 5. PSNR (dB) of the denoised images with mixed noise

Images	Adaptive median filter	Bilateral filter	[3]	Our method
1	36.06	24.70	26.87	41.22
2	36.28	25.41	31.32	42.05
3	36.19	24.92	30.04	41.83
4	35.68	25.10	30.04	37.80
5	35.41	25.53	31.66	39.55
Average	35.92	25.13	29.99	40.49

Table 6. SSIM of the denoised images with mixed noise

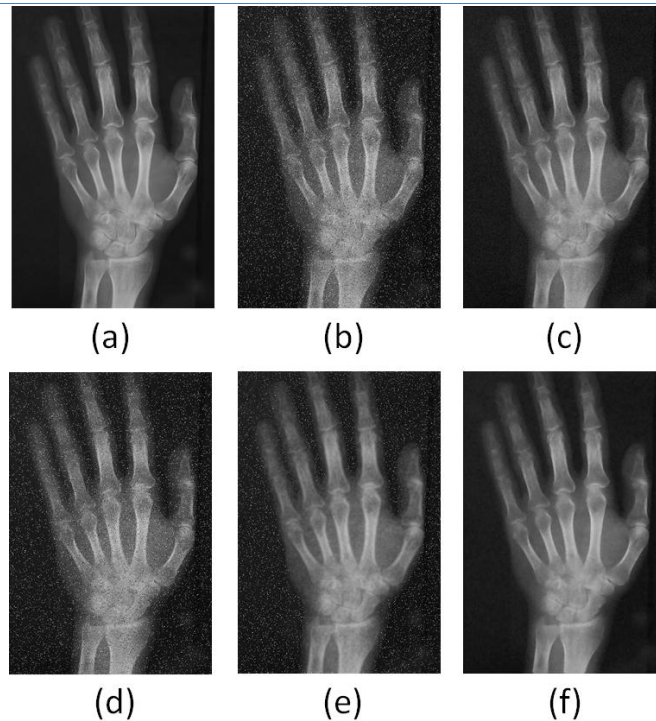| Images	Adaptive median filter	Bilateral filter	[3]	Our method
1	0.8395	0.7126	0.8216	0.9684
2	0.8144	0.6418	0.8692	0.9368
3	0.8408	0.6771	0.8882	0.9617
4	0.8417	0.6762	0.8329	0.9019
5	0.8481	0.6911	0.9158	0.9657
Average	0.8369	0.6798	0.8655	0.9469

Figure 5. The denoised results. (a) The original image. (b) The image with mixed noise. (c) Image denoised by adaptive median filter. (d) Image denoised by bilateral filter. (e) Image denoised by [3] (f) Image denoised by our method.

3.3   Evaluation of contrast enhancement

A typical way to compare the contrast enhancement is visual evaluation. Figure 6 shows the enhanced images of different methods. We can observe that the AHE results in over-contrast images, which is not the desired results; on the contrary, CLAHE and our method are able to obtain visually satisfactory results. By applying the mathematical morphology before contrast enhancement, our method can obtain more details such as edges and textures than the CLAHE.
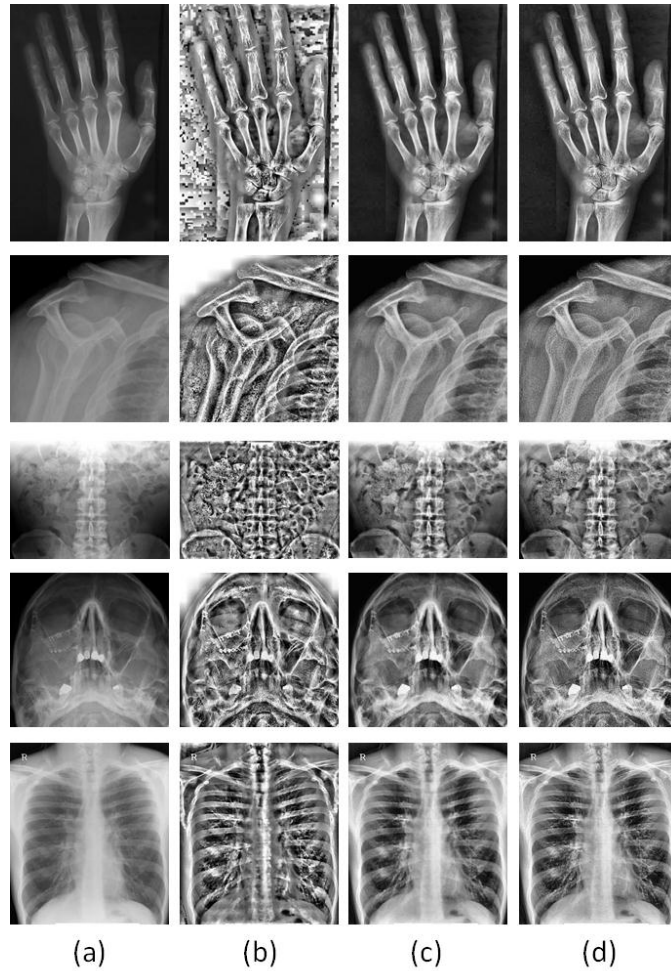
(a)   (b)   (c)   (d)

Figure 6. The images enhanced by different methods. (a) The original images. (b) The results of AHE. (c) The results of CLAHE. (d) The results of our method.

To evaluate the contrast enhancement objectively, we applied the "absolute mean brightness error" (AMBE) [22] as the quantitative index to compare the results of different methods. The AMBE is defined as follows:

$$AMBE = \frac{1}{N}\sum_{i=1}^{N}\left|\bar{I}_i - \bar{O}_i\right| \tag{11}$$

where N is the number of pixels in the image; $\bar{I}_i$ and $\bar{O}_i$ are the mean values of a local window with size 5 × 5 centered at i-th pixel in the enhanced image and original image, respectively. The AMBE computes the averaged difference of mean brightness between the original image and the enhanced one. Ideally, the contrast enhancement should preserve the same mean brightness of an image. Therefore, the lower AMBE represents less brightness bias. Table 7 shows that the AHE has much higher AMBE than the CLAHE and our method since the over-contrast problem in the homogeneous regions. Our method obtained only slightly higher AMBE than CLAHE, therefore, we need another index, EME, to compare the performance of contrast enhancement.

Table 7. AMBE of the different methods for contrast enhancement			
Images	AHE	CLAHE	Our method
1	82.4412	22.3001	24.0573
2	59.5952	18.5297	19.2049
3	61.6608	27.9984	29.7133
4	62.9189	30.3828	32.5923
5	45.3140	19.0869	19.8624
Average	62.3860	23.6596	25.0860

Table 8. EME comparisons			
Images	Original image	CLAHE	Our method
1	15.5255	28.5173	34.3282
2	12.2870	19.0951	24.1989
3	10.8004	23.4589	29.2741
4	22.5410	35.9354	46.9401
5	14.8050	26.7551	33.2626
Average	15.5255	28.5173	34.3282

The EME is defined as follows:

$$EME = \frac{1}{K}\sum_{i=1}^{K}\left(20\cdot\ln\left(\frac{I_{i,max}}{I_{i,min}}\right)\right) \tag{12}$$

where the image is divided into K non-overlapping blocks with equal size m × m (we set m = 32 in this paper), $I_{i,max}$ is the maximum value of the i-th block, and $I_{i,min}$ is the minimum value of the i-th block.

The EME averages the contrast of all the local regions to represent the contrast of whole image, which means the higher EME, the better contrast of image. Table 8 shows that our method obtained the images with significantly higher EME than the original images and the images enhanced by CLAHE.

4   Conclusions

In this paper, we have proposed an algorithm with capability of noise reduction and contrast enhancement for X-ray images. The noise reduction part combines the adaptive median filters and bilateral filter to deal with the mixed noise. Then we apply the mathematical morphology followed by CLAHE to enhance the contrast with more details such as edges. The experiments show that our method is able to obtain averaged PSNR 40.49 dB and averaged SSIM 0.9469 in the mixed noise case; for the contrast enhancement, our method is able to obtain higher EME values than CLAHE, which means the images enhanced by our method have better contrast than the images enhanced by CLAHE.

REFERENCES

[1].   Langland, O.E., et al., *Principles of Dental Imaging*. Lippincott Williams & Wilkins, 2002.

[2].   Ito, K. and Xiong, K., *Gaussian filters for nonlinear filtering problems*. Automatic Control, IEEE Transactions on, 2000. 45(5): p. 910-927.

[3].   Kurt, B., et al., *Medical images enhancement by using anisotropic filter and clahe*. In Innovations in Intelligent Systems and Applications (INISTA), 2012 International Symposium On, 2012. p. 1-4.

[4].   Perona, P. and Malik, J., *Scale-space and edge detection using anisotropic diffusion*. Pattern Analysis and Machine Intelligence, IEEE Transactions on, 1990. 12(7): p. 629-639.

[5].   Yu, Y. and Acton, S.T., *Speckle reducing anisotropic diffusion*. Image Processing, IEEE Transactions on , 2002. 11(11): p. 1260-1270.

[6].   Paris, S., et al., *A gentle introduction to bilateral filtering and its applications*. In ACM SIGGRAPH 2007 Courses, 2007.

[7].   Tomasi, C. and Manduchi, R., *Bilateral filtering for gray and color images*. In Computer Vision, Sixth International Conference On, 1998. p. 839-846.

[8].   Lin, H.-M. and Willson Jr, A.N., *Median filters with adaptive length*. Circuits and Systems, IEEE Transactions on, 1988. 35(6): p. 675-690.

[9].   Ko, S.-J. and Lee, Y.H., *Center weighted median filters and their applications to image enhancement*. Circuits and Systems, IEEE Transactions on, 1991. 38(9): p. 984-993.

[10].   Tsai, C.-Y., *An adaptive rank-ordered median image filter for removing salt-and-pepper noise*. Master's thesis, National Cheng-Kung University, 2006.

[11].   Hwang, H., et al., *Adaptive median filters: new algorithms and results*. Image Processing, IEEE Transactions on, 1995. 4(4): p. 499-502.

[12].   Lehr, J. and Capek, P., *Histogram equalization of ct images*. Radiology, 1985. 154(1): p. 163-169.

[13].   Khalid, N.E.A., et al., *Cr images of metacarpel cortical edge detection-bone profile histogram approximation method*. In Intelligent and Advanced Systems (ICIAS), International Conference On, 2007. p. 702-708.

[14].   Wang, Y., et al., *Image enhancement based on equal area dualistic sub-image histogram equalization method*. Consumer Electronics, IEEE Transactions on, 1999. 45(1): p. 68-75.

[15].   Pizer, S.M., et al., *Adaptive histogram equalization and its variations*. Computer vision, graphics, and image processing, 1987. 39(3): p. 355-368.

[16].   Stark, J.A., *Adaptive image contrast enhancement using generalizations of histogram equalization*. Image Processing, IEEE Transactions on, 2000. 9(5): p. 889-896.

[17].   Sund, T. and Møystad, A., *Sliding window adaptive histogram equalization of intraoral radiographs: effect on image quality*. Dentomaxillofacial Radiology, 2014.

[18].   Kim, Y.-T., *Contrast enhancement using brightness preserving bi-histogram equalization*. Consumer Electronics, IEEE Transactions on, 1997. 43(1): p. 1-8.

[19].   Shoaib, M., et al., *Design and implementation of efficient information retrieval algorithm for chest x-ray images*. Journal of American Science, 5(4): p. 43-48.

[20].   Sund, T. and Eilertsen, K., *An algorithm for fast adaptive image binarization with applications in radiotherapy imaging*. Medical Imaging, IEEE Transactions on, 2003. 22(1): p. 22-28.

[21].   Noor, N.M., et al., *Fish bone impaction using adaptive histogram equalization (ahe)*. In Computer Research and Development, 2010 Second International Conference On, 2010. p. 163-167.

[22]. Ibrahim, H. and Kong, N.S.P., *Brightness preserving dynamic histogram equalization for image contrast enhancement*. Consumer Electronics, IEEE Transactions on, 2007. 53(4): p. 1752-1758.

[23]. Yang, Y., et al., *Medical image enhancement algorithm based on wavelet transform*. Electronics letters , 2010. 46(2): p. 120-121.

[24]. Shrimali, V., et al., *Comparing the performance of ultrasonic liver image enhancement techniques: a preference study*. IETE Journal of Research, 2010. 56(1): p. 4-10.

[25]. Gonzalez, R.C. and Woods, R.E., *Digital Image Processing (3rd Edition)*. Prentice-Hall, Inc., Upper Saddle River, NJ, USA, 2006.

[26]. Mahmoud, T.A. and Marshall, S., *Medical image enhancement using threshold decomposition driven adaptive morphological filter*. In 16th European Signal Processing Conference (EUSIPCO), 2008.

[27]. Agaian, S.S., et al., *Transform-based image enhancement algorithms with performance measure*. Image Processing, IEEE Transactions on, 2001. 10(3): p. 367-382.